ELSEVIER

International Journal of Heat and Fluid Flow 23 (2002) 330–339

International Journal of HEAT AND FLUID FLOW

www.elsevier.com/locate/ijhff

Comparison of numerical methods applied to the flow over wall-mounted cubes ☆

Stefan Schmidt [a,*], Frank Thiele [b]

[a] CSIRO Division of Building, Construction and Engineering, P.O. Box 56, Highett, Vic. 3190, Australia
[b] Hermann–Föttinger-Institute for Fluid Mechanics, Technical University of Berlin, 10623 Berlin, Germany

Abstract

Latest developments in the simulation of turbulence by detached eddy simulation (DES) have suggested that this technique might be able to replace large eddy simulation (LES) within the next decade. The results of the flow past a square cylinder show that this approach is quite inexpensive compared to LES while capturing the most important features of the flow. This study extends the range of applications of DES towards a fully unsteady three-dimensional case with strong streamline curvature, which is known to be a major problem for Reynolds-averaged Navier–Stokes equation (RANS) methods. The case considered is the turbulent flow over wall-mounted cubes at a Reynolds number of $Re = 1.3 \times 10^4$. The results demonstrate that DES is able to capture the most dominant flow patterns like LES, while RANS only gives a only a poor representation of the unsteady flow phenomena. © 2002 Published by Elsevier Science Inc.

Keywords: Turbulence modeling; Wall-mounted cubes; LES; DES; RANS

1. Introduction

In the past, the Reynolds-averaged Navier–Stokes equation (RANS) seemed to be the only way to calculate turbulent flows of industrial relevance. However, large eddy simulation (LES) has recently become very popular, but currently appears not to be able to fulfil the promise to be the adequate tool for computational fluid dynamics in the future. This is basically due to the absence of universal wall functions, which would allow for a reduction of grid points in the near-wall region and the simplicity of present subgrid-scale modeling, which is not able to capture all relevant flow phenomena with sufficient accuracy. Hence, LES demands very fine near-wall resolution to directly resolve the turbulent structures. For this reason, wall-resolving LES remains fairly time consuming, disqualifying this method for industrial applications especially at higher Reynolds numbers.

Most recently, detached eddy simulation (DES) has become a promising tool for the prediction of turbulence. Besides other approaches to combine RANS with the quality of flow predictions by wall-resolving LES, this method avoids the high near-wall resolution by applying RANS in the vicinity of the wall and employing a modification of the Spalart–Allmaras one-equation turbulence model in the far field. In the overlap region, this model blends automatically from a statistical turbulence model to a subgrid-scale model without the use of shape functions. Since RANS calculations often fail to capture unsteady flow phenomena, which are present behind bluff-bodies (e.g. cubes) or airfoils at high angles of attack, the main advantage of DES arises from the fact that it captures unsteady flow regions such as wakes and recirculation zones.

This study aims at validating this fairly new technique and wants to shed light on its physical limitations in comparison to wall-resolving LES and RANS. The main intention of this paper is to investigate the level of three dimensionality in terms of spatial resolution is required for DES in order to still outperform RANS results and to get the dominant unsteady flow features and

☆ This paper is a revised and expanded version of a paper presented at CHT'01, the Second International Symposium on Advances in Computational Heat Transfer (Palm Cove, Qld., Australia, 20–25 May 2001), the proceedings of which were published by Begell House, Inc.

* Corresponding author. Tel.: +61-3-9252-6195; fax: +61-3-9252-6240.

E-mail address: stefan.schmidt@csiro.au (S. Schmidt).

0142-727X/02/$ - see front matter © 2002 Published by Elsevier Science Inc.
PII: S0142-727X(02)00180-7

satisfactory results, which favourably compare to LES results on the other hand.

2. Simulation of turbulence

As this paper focuses on the comparison of different numerical techniques to simulate turbulent flows, LES and DES are briefly described in the following paragraph. For RANS, we refer to literature (Pope, 2000; Wilcox, 1993).

2.1. Large eddy simulation

In LES, only the large scales are explicitly resolved by the numerical grid while the smaller ones are represented by a subgrid-scale model. The motivation for this approach is that the large-scale vortices are dominated by geometrical constraints and boundary conditions. Due to turbulent transport phenomena these vortices pass their kinetic energy on towards smaller vortices while the orientation of the initial vortices gets lost during this energy cascade. Therefore, the small-scale turbulence is expected to be isotropic without any preferred orientation and should consequently be much easier to model than the whole spectrum of turbulence.

Starting with the governing equations for an incompressible three-dimensional (3D) unsteady flow field

$$\begin{aligned}&\frac{\partial u_k}{\partial x_k}=0,\\&\frac{\partial u_i}{\partial t}+\frac{\partial (u_i u_j)}{\partial x_j}=-\frac{1}{\rho}\frac{\partial p}{\partial x_i}+\frac{\partial}{\partial x_j}\left[\nu\left(\frac{\partial u_i}{\partial x_j}+\frac{\partial u_j}{\partial x_i}\right)\right],\end{aligned}\tag{1}$$

we apply a top-hat filter function $\overline{G(\mathbf{x},\mathbf{x}')}$

$$\begin{aligned}&\bar{u}_i(\mathbf{x})=\int_\Omega \overline{G(\mathbf{x},\mathbf{x}')}u_i(\mathbf{x}')\,\mathrm{d}\mathbf{x}',\\&\overline{G(\mathbf{x},\mathbf{x}')}=\begin{cases}1, & |\mathbf{x}-\mathbf{x}'|<\Delta/2,\\ 0, & \text{all other cases}\end{cases}\end{aligned}\tag{2}$$

to separate large and small-scale motion leading to the filtered equation set

$$\begin{aligned}&\frac{\partial \bar{u}_k}{\partial x_k}=0,\\&\frac{\partial \bar{u}_i}{\partial t}+\frac{\partial (\overline{u_i u_j})}{\partial x_j}=-\frac{1}{\rho}\frac{\partial \bar{p}}{\partial x_i}+\frac{\partial}{\partial x_j}\left[\nu\left(\frac{\partial \bar{u}_i}{\partial x_j}+\frac{\partial \bar{u}_j}{\partial x_i}\right)\right].\end{aligned}\tag{3}$$

The correlation within the convective term ($\overline{u_i u_j}$) is a priori unknown and has to be modeled. The most common way is to rewrite this term to

$$\tau_{ij}=\overline{u_i u_j}-\bar{u}_i\bar{u}_j \tag{4}$$

and split the additional stresses into an anisotropic part $\tau_{ij}^{\mathrm{a}}=\tau_{ij}-1/3\,\tau_{kk}\delta_{ij}$ and add the isotropic fraction to the pressure $p^*=\bar{p}+1/3\,\tau_{kk}$, leading to the LES equation set, forming the basis of this investigation

$$\frac{\partial \bar{u}_k}{\partial x_k}=0, \tag{5}$$

$$\frac{\partial \bar{u}_i}{\partial t}+\frac{\partial (\bar{u}_i\bar{u}_j)}{\partial x_j}=-\frac{1}{\rho}\frac{\partial p^*}{\partial x_i}+\frac{\partial}{\partial x_j}\left[\nu\left(\frac{\partial \bar{u}_i}{\partial x_j}+\frac{\partial \bar{u}_j}{\partial x_i}\right)\right]-\frac{\partial \tau_{ij}^a}{\partial x_j}. \tag{6}$$

2.2. Subgrid-scale models

The most commonly known model is the Smagorinsky model (Smagorinsky, 1963), which is based on a simple mixing-length approach. It includes one parameter (C_{S}) which has to be fixed according to the flow problem and is usually be taken to $C_{\mathrm{S}}=0.1$ for most turbulent flows. Under strong shear this parameter has to be reduced and near rigid walls a Van Driest damping function (Van Driest, 1956) must be introduced to ensure the correct wall development by dampening out the eddy viscosity.

The dynamic procedure (Germano et al., 1991; Lilly, 1992) overcomes this parameter problem as it extracts a time-dependent mixing-length from the filtered velocity field and evaluates a local parameter $C(x,y,z,t)$. This important feature avoids the a priori determination of the mixing-length in terms of the model parameter and makes this model sensitive to the local turbulence structure. Hence, the dynamic model (DM) is able to switch off in laminar or fully resolved flow regions. Additionally, this model is capable of predicting backscatter in terms of negative values of the mixing-length and consequently of the eddy viscosity. Despite the fact that the DM avoids the parameter problem, the procedure suffers from numerical difficulties possibly destabilizing the calculation and leading to divergence. However, in the presence of homogeneous directions, these shortcomings can be suppressed by averaging the parameter in these directions.

The more elaborate dynamic one-equation model (DOEM) (Davidson, 1997) employs the turbulent subgrid kinetic energy to avoid these aforementioned numerical difficulties associated with all DMs, while retaining the key features of the dynamic approach. This model remains stable also in complex geometries without any homogeneous directions and is in this sense superior to the standard model. The favourable stability properties as compared to the DM usually outweigh the higher computational costs of solving the additional transport equations.

The higher demand of computer resources introduced by dynamic modeling is more than justified, as the Smagorinsky requires the knowledge of the local wall shear stress to ensure the correct near-wall behaviour and the adequate level of dissipation to give satisfactory results. The advantage of the DM is the property that it

does not require *any* adjustments prior to the simulation.

2.3. Detached eddy simulation

DES (Spalart et al., 1997) takes advantage of the RANS method where the mean flow remains attached and steady (e.g. walls) while offering, like LES, the sensitivity to capture unsteady flow phenomena in areas of physical interest such as wakes or recirculation zones. Although this method is beyond the computational costs of a steady two-dimensional (2D)-RANS calculation, it reveals nearly as much information of the flow dynamics as LES. For this reason, DES could be a promising way out of the limitation detaining LES from being applied to high Reynolds numbers.

The DES methodology is basically a modification of the dissipation term within the Spalart–Allmaras one-equation turbulence model (Spalart and Allmaras, 1994). This term is strongly affected by the wall-normal distance d, which is substituted by a new length scale $\tilde{d}$ (Shur et al., 1999)

$$\tilde{d} = \min(d, C_{\mathrm{DES}}\Delta), \quad C_{\mathrm{DES}} = 0.65, \tag{7}$$

which defines the border between RANS and LES. For small values of the wall distance, where $d < C_{\mathrm{DES}}\Delta$ (e.g. in boundary layers), the original model will hold. In the far field $d > C_{\mathrm{DES}}\Delta$ the length-scale approaches the local grid size Δ, for which the maximum of Δ_x, Δ_y, Δ_z is taken. This makes the SA-model act as a subgrid-scale model with a mixing-length equal to the grid spacing. Note that this is in contrast to the usual practice in LES, wherein an average cell volume $\Delta = (\Delta_x\Delta_y\Delta_z)^{1/3}$ is used.

As RANS remains attractive to simulate a wide range of turbulent flows, the results of unsteady calculations with an algebraic stress model (EASM), which is basically a non-linear eddy-viscosity model, is also included.

3. Numerical scheme

The flow solver ELAN3D (Xue, 1998) is based on an implicit pressure-based finite volume Navier–Stokes procedure applying a cell-centred discretisation on semi-structured grids. The scheme uses a pressure correction scheme and a generalised Rhie and Chow (1983) interpolation to avoid a de-coupling between velocity and pressure. The code is second-order accurate in space and time and uses multi-block algorithms. Several upwind-biased limited HOC schemes are available, which are only used in the context of DES and RANS. They ensure a higher approximation order of the convective terms on coarse meshes, which are usually employed by RANS/DES compared to LES. In the far field, the inherent numerical diffusion of the convection scheme retains numerical stability without sacrificing the loss of resolved dynamics in areas close to the airfoil (e.g. wake). For LES, only the symmetric convection scheme CDS-2 is applied. Furthermore, the solver has been parallelised using domain decomposition, where the performance has been quantified to roughly 60 MFLOPs per processing element on a CRAY T3E-900.

4. Flow past a square cylinder

A suitable testcase to work out the differences between LES and DES is the turbulent flow over a square cylinder, which is considered to be a key flow configuration for the validation of turbulence models. The oncoming laminar flow is impinging on the cylinder front and separating at the leading edges. The flow undergoes transition to turbulence in the separated shear layers and forms a vortex street in the wake due to periodic vortex shedding at the lee side of the cylinder. The typical shedding frequency is characterised by the Strouhal number ($St = fD/U_\infty$), normalised by the cylinder diameter D and the flow speed U_∞. The flow domain and the Reynolds number ($Re = 22000$) are set according to the experiment (Lyn et al., 1995).

Although this test case is rather simple in geometry and has a fixed geometry-induced separation, this flow features an unsteady wake, which turned out to render difficulties for RANS based models usually leading to a under representation of the transient motion. Therefore, the aim of this validation is to investigate whether switching to DES automatically leads to superior results when run on the *same* grid as RANS. Furthermore, a grid study based on DES is performed to find out how much three dimensionality has to be directly resolved by the mesh to achieve acceptable results or from an opposite point of view, to help getting an idea of the minimum spanwise resolution required to predict the main features of the 3D flow. Recent LES results based on the DOEM (Table 1) are added for reference and were previously compared to results of the ERCOFTAC workshop (Rodi et al., 1997).

All simulations make use of the same block-structured grid in the cross-sectional (x, y) plane which consists of about $N_{2D} = 32000$ grid points. The wall-normal distance of the first mesh point around all cylinder walls was set to $\delta/D = 0.0064$ being smaller than the value $\delta/D = 0.0080$ taken by (Sohankar et al., 2000). In order to demonstrate the influence of the spanwise discretisation, different numbers of grid points (NK) to resolve this direction (z) are used (Table 1). While the LES case uses NK = 32 points, the DES cases employ NK = 20 (DES-A), NK = 10 (DES-B) and NK = 2 points (DES-C), respectively. Note that the latter is applied to a smaller spanwise domain to prevent the rise of numerical oscillations owing to extreme cell aspect ratios in that direction. This simulation (DES-C) is performed on a

Table 1
Global parameters of square cylinder flow

	CPU $\sim h/T^*$ ($T^* = D/U_*$)	NK	Δ_z	St	l_r	$\bar{c}_d$	c'_d	c'_l
EXP[a]	–	–	–	0.132	1.38	2.1	–	–
LES-OEDSM[b]	–	25	0.167	0.130	–	2.25	0.20	1.50
LES-DOEM[c]	66 h	32	0.125	0.13	1.07	2.18	0.19	1.47
DES-A	41 h	20	0.200	0.13	1.16	2.42	0.28	1.55
DES-B	21 h	10	0.400	0.10	1.37	2.48	0.54	1.36
DES-C	4 h	2	0.500	0.09	1.36	2.57	0.68	1.39
RANS-EASM[d]	4 h	2	0.500	0.15	1.64	2.21	0.08	0.95

[a] Lyn et al. (1995).
[b] Sohankar et al. (2000).
[c] Schmidt (2000).
[d] Schmidt et al. (1999).

typical 2D mesh and therefore comparable to an unsteady RANS calculation, it requires only 6% of the computing time of the LES. The comparative run with the EASM was carried out on the same mesh as the DES-C and made use of wall functions.

The global parameters (Table 1) give an impression of the dynamical behaviour of the flow. A decrease in the spanwise resolution results in a loss of unsteady motion represented by the Strouhal number which drops from 0.13 (LES) to 0.09 (DES-C). At the same time, the predicted size of the recirculation zone l_r increases as can also be seen in Fig. 1(a). This is basically due to a reduction of momentum exchange in the under resolved spanwise direction, leading to a quasi-2D flow field. The mean drag coefficient $\bar{c}_d$ and its fluctuating component c'_d increase due to a loss in three dimensionality, while the lift fluctuations c'_l retain their magnitudes ($c'_l = 1.4$–1.5). In order to assess the performance of the DOEM, comparable LES results with a DOEM (Sohankar et al., 2000) are shown, indicating a good agreement for all given parameters. Remaining deficiencies can be attributed to the local grid spacing in the cross-sectional plane and in the spanwise direction, since both used a comparable numerical methods of the same accuracy. From the LES and DES results it becomes evident that a larger recirculation length l_r usually reduces the shedding frequency St. The additional RANS results, obtained with a non-linear eddy-viscosity model, however, show a contrary behaviour: both quantities l_r and St are higher than the corresponding LES and DES values.

A closer look at the centreline profiles of the mean velocity (Fig. 1(a)) reveals that both LES and DES-A yield nearly the same back-flow component at $x < 2$, while the latter over predicts the velocity in the wake $x > 3$. Compared to case DES-A, the coarse-grid simulations DES-B/C result in a much better prediction of both mean recirculation length and wake region, which almost matches the LES and experimental data. From the velocity fluctuations (Fig. 2(a) and (b)), it can be seen that the reduction of the spanwise resolution leads

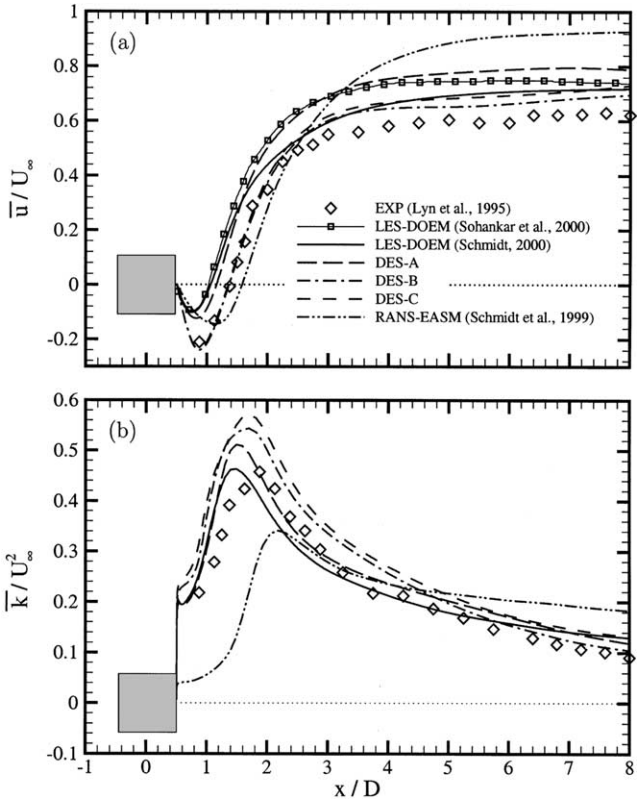

Fig. 1. Square cylinder flow: (a) mean streamwise velocity and (b) total kinetic energy.

to a strong increase of the streamwise stress component $\overline{u'u'}/U_\infty^2$ and a decrease of the spanwise component $\overline{w'w'}/U_\infty^2$, which vanishes completely for DES-C (Fig. 2(a)). The dominating cross-flow stress component $\overline{v'v'}/U_\infty^2$ (Fig. 1(b)) is rather insensitive to the spanwise resolution and therefore predicted at nearly the same magnitude by all simulations, which leads only to a small rise of the turbulent kinetic energy $\overline{k}/U_\infty^2$ (Fig. 1(b)). The EASM shows the typical behaviour of the RANS approach, as the dynamic properties of the flow

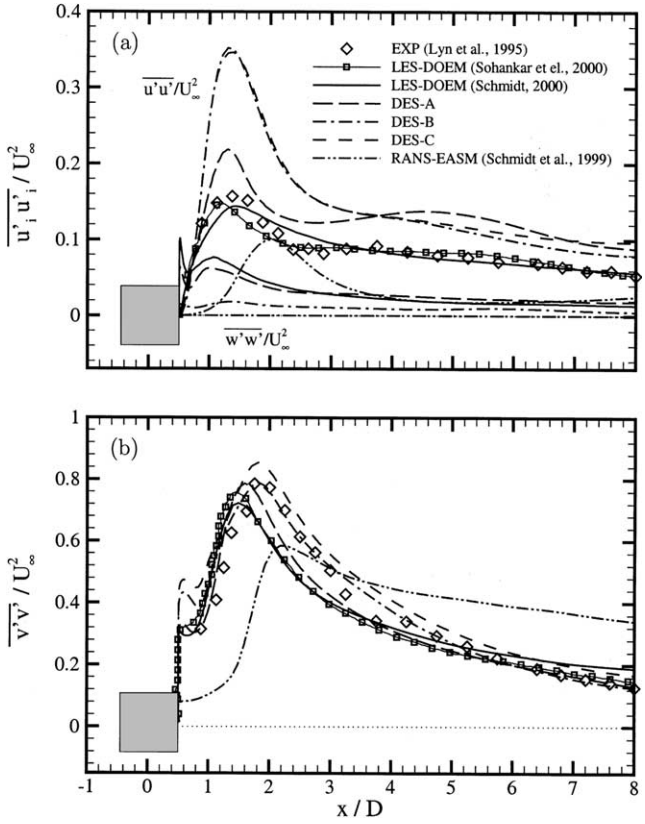

Fig. 2. Square cylinder flow: (a) total normal stress in the stream- and spanwise and (b) in the cross-flow direction.

in terms of Reynolds-stress levels are under predicted. Compared to the DES-C, the EASM achieves only poor results with distinct differences in all quantities. It turns out that even a DES on a 2D-mesh outperforms a sophisticated non-linear eddy-viscosity model, like the EASM (Schmidt et al., 1999).

5. Flow over wall-mounted cubes

The considered flow is the turbulent flow over an array of wall-mounted cubes in a channel. The Reynolds number based on the mean velocity U_b and the cube size H equals $Re = 1.3 \times 10^4$. The geometry of the testcase, which has already been the subject of the ERCOFTAC workshop in Helsinki (Hellsten and Rautaheimo, 1999) is shown in Fig. 3. The computational domain covers the area from $0 < x < S$, $-S/2 < y < +S/2$ and $0 < z < h = 3.4H$ and is a subset of the total experimental setup of Meinders (1998), who experimentally investigated an array of cubes. As the main intention of this paper was an assessment of numerical techniques for calculating turbulent flows based on a 3D geometry, the heat transfer was not accounted for.

The previous validation suggested that DES can be successfully carried out on coarse RANS meshes and is able to achieve satisfactory results compared to LES. Although the flow over wall-mounted cubes is a true 3D configuration, it offers similar features as the flow around a square cylinder such as a fixed geometry-induced separation and an expected unsteady recirculation zone between two following cubes. As DES is applied to a RANS mesh and aiming to resolve the turbulent structures like LES, the DES results are expected to be worse than the LES ones in the interior part of the domain and similar to RANS close to the walls. On the other hand, using the same amount of grid points as LES would reduce the savings of the DES compared to RANS significantly. Therefore, the DES is carried out on the same mesh as RANS to get a comparable response of the quality of DES on a fairly coarse mesh. The numerical grid consists of a block-structured mesh containing roughly 800 000 and 120 000 cells for the LES and DES/RANS respectively. The cube wall-normal distance is kept within a range of $\delta n \approx 0.007H$ (LES) and $\delta n \approx 0.015H$ in case of the DES/RANS, which is in the range of contributions of the workshop (Hellsten and Rautaheimo, 1999).

5.1. Boundary conditions

To allow for a comparison with the experimental data (Meinders, 1998), periodic boundary conditions are used for both streamwise (x) and spanwise (z) directions. All other faces are treated as fixed walls employing the no-slip condition for LES and wall functions for DES/RANS. The flow is forced by a pressure gradient which is generated by a pressure difference ΔP. Since there is no exact relation between the friction and and the pressure force, the exact pressure difference is part of the solution. In a prior steady RANS calculation, this pressure is estimated and afterwards used as an input parameter for the periodic simulations (LES/DES). Additionally, the required mass flux $\Phi = 6.85 \times 10^{-3}$ kg s^{-1} is ensured by adapting the pressure gradient during the calculation by comparison of the actual and desired mass flux at each time-step and adapting the pressure force successively until the right pressure has been found. After that initial process, the simulation has been advanced over $t^* \approx 10tU_b/H$ convective time units to get rid of any initial conditions.

6. Results

Since RANS predicts a steady flow field, only time-averaged quantities are presented for LES/DES. The results of all numerical approaches are compared to the measurements of Meinders (1998). The streamline patterns (Fig. 4) give an impression of the flow behaviour in

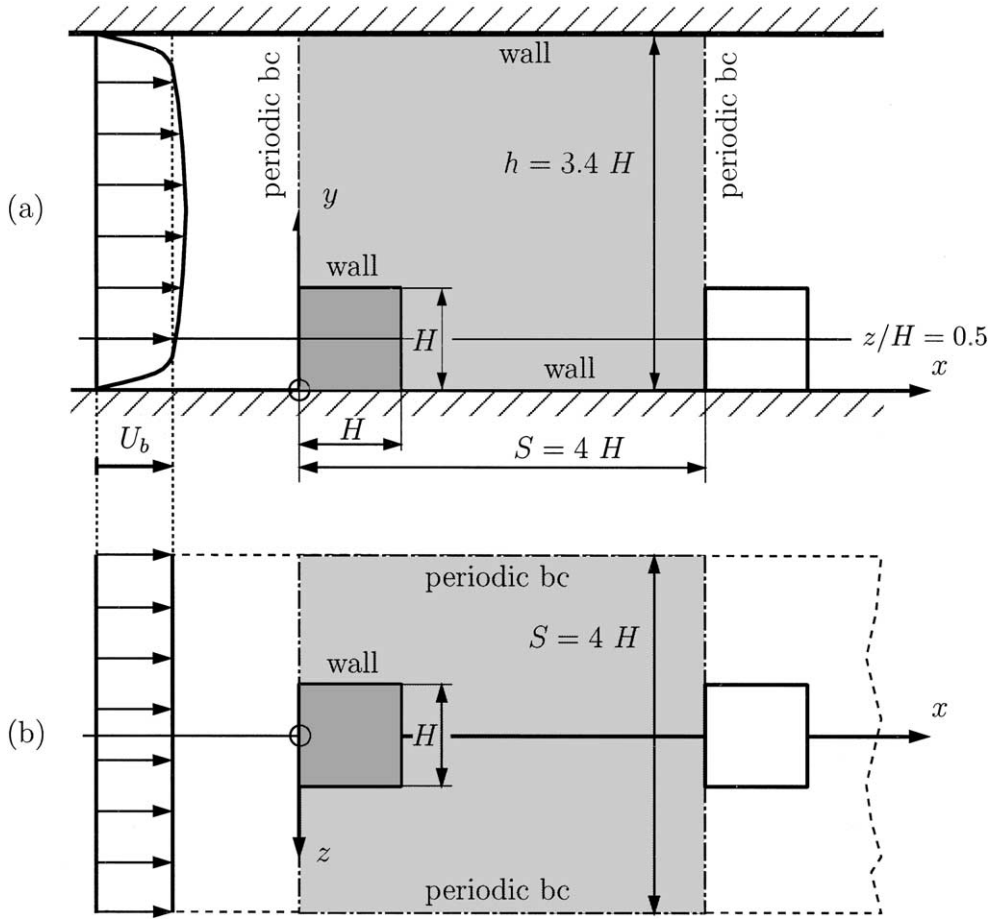

Fig. 3. Wall-mounted cubes: boundary conditions and geometry; (a) x, y-plane and (b) x, z-plane.

the considered domain. In the plane $z/H = 0.0$, both LES and DES form a weak rear-corner vortex and one major front vortex, while in the RANS calculation a strong arch vortex downstream of the cube dominates the flow in the recirculation area. At half cube height $y/H = 0.5$, the streamline pattern indicate a non-symmetric distribution in the recirculation area for all simulations. For LES and DES this can be attributed to the non-settled statistics of the mean velocities while for the RANS this effect is due to a lack of three dimensionality, which consequently limits the turbulent mixing.

6.1. Mean velocities

The numerical and experimental data at five locations $x/h = 0.3$, 0.7, 1.3, 1.7, 2.3, 3.7 downstream of the cube are shown on the planes $z/H = 0.0$ and $y/H = 0.5$ (Fig. 5). As expected, all results achieve a reasonable agreement with the measurements, showing only minor differences in the mean recirculation zone between both cubes. In that region, only LES is able to capture the correct velocity profile. Both DES and RANS over predict the height and the spanwise extent of the recirculation zone.

6.2. Fluctuating velocities

The Reynolds-stress levels of $\overline{u'u'}/U_b^2$ (Fig. 6(a) and (b)) show that LES is able to capture the main flow physics correctly. However, on both cutting planes at all locations too large stress values are obtained revealing an insufficient spatial resolution in the region of the separated shear layer around the cube ($y/H \approx 1$, $z/H \approx \pm 0.5$). The DES results obtained on an even coarser mesh are worse and exceed the LES ones by more than a factor of two. This is due to the low resolution of the DES mesh compared to the LES mesh in the separating shear layer. The DES is basically designed to work like a LES on a RANS grid and therefore the DES is not able to resolve the turbulent structures like LES. This is apparently in contrast to the flow past the square cylinder, where even on a very coarse mesh the fluctuating velocities were quite satisfactory. It is known that under resolved simulations of turbulence usually predict *higher* velocity fluctuations in

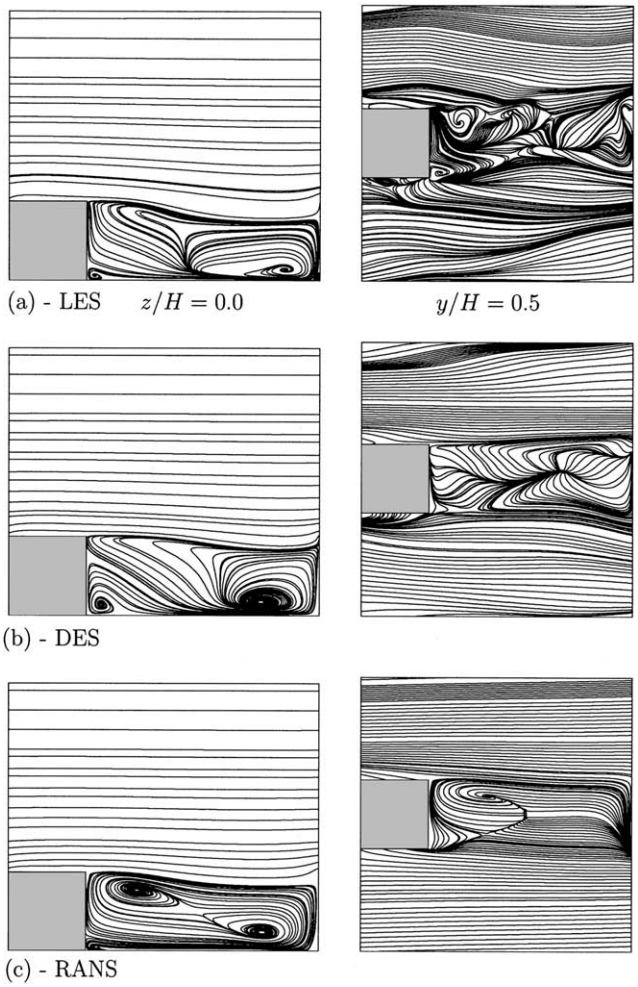

Fig. 4. Time-averaged streamlines of LES (a), DES (b) and RANS (c) on the z-plane and y-plane.

the mean flow direction (x) and *smaller* values in the cross-flow direction (y, z). This has happened in case of the DES (see Fig. 6(c)–(f)). The spanwise stress component $\overline{w'w'}/U_b^2$ (Fig. 6(e) and (f)) is under predicted by both LES and DES. In terms of the stress level, the RANS results do a better job, however, predicting a different shape of the profiles, especially near the upper channel wall, where a local stress maximum is visible and in the recirculation zone, where the results suffer from a misinterpretation of the flow structures. Unfortunately, no experimental data are available for the wall-normal stress component $\overline{v'v'}/U_b^2$ (Fig. 6(c) and (d)). Comparing the shape of $\overline{v'v'}/U_b^2$ with the previous discussed stress $\overline{w'w'}/U_b^2$, it is most likely that the stress is also under resolved by LES and DES while the RANS result fails to capture the shape of the profile once more. Note that all Reynolds stresses are predicted remarkably well by RANS outside the important recirculation zone and the upper channel wall—in particular $\overline{u'u'}/U_b^2$ (Fig. 6(a) and (b)). Apparently, the EASM, which is basically a non-linear k–ε model, employed in the RANS calculation is not very suitable for that kind of flow, although the included curvature terms should have a positive effect on the flow prediction. The results of the workshop (Hellsten and Rautaheimo, 1999) indicate that ω-based RANS models compare reasonably well with the measurements while models based on ε seem to give poor results.

From the active shear stresses $\overline{u'v'}/U_b^2$ and $\overline{u'w'}/U_b^2$ (Fig. 7(a) and (b)) only minor variations can be seen. Like the cross-flow normal stresses (see Fig. 6(c)–(f)), the shear stresses tend to be under estimated showing lower values for the DES compared to the LES. The shear stress level predicted by RANS are of the same magnitude as the LES ones with slightly different shape owing to the principle differences of the models used.

7. Conclusions

In this paper different numerical approaches, namely LES, DES and RANS were applied to the flow past a square cylinder and over wall-mounted cubes. The main intention of this investigation was to assess of the performance of DES compared to LES and RANS on a given coarse mesh *without* aiming to achieve perfect

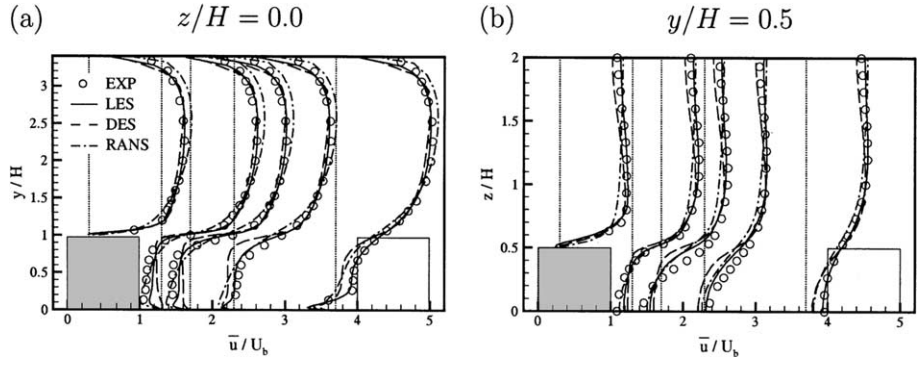

Fig. 5. Mean streamwise velocity $\overline{u}/U_b$ on the z-plane (a) and y-plane (b).

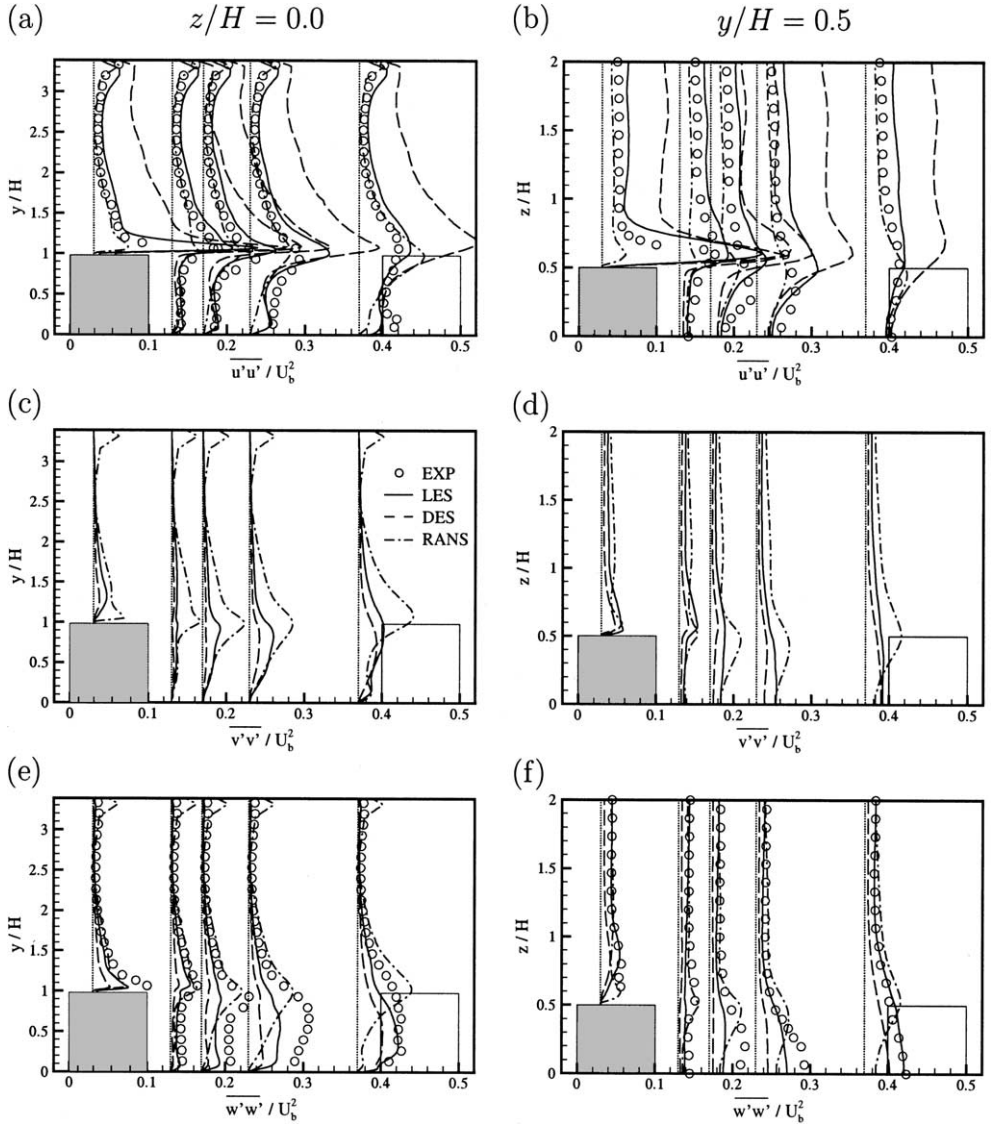

Fig. 6. Reynolds normal stresses $\overline{u_i'u_i'}/U_b^2$ on the z-plane (a) and y-plane (b).

agreement of any of the solutions with reference data but to investigate the advantages and limitations of this fairly new approach. DES is an alternative to pure RANS and LES. It is a combination of both incorporating the advantages to capture unsteady flow features like LES and being reasonably cheap in terms of computing resources like RANS.

The outcome of this study is twofold. The flow past the square cylinder has revealed that a coarse approximation of the spanwise direction reduces the resolved stress levels and the dynamics of the vortex shedding, but has only a minor influence on the mean velocity profiles. Therefore only the wall region has to be of major concern when creating a mesh. On the other hand, the simulation of the flow around the wall-mounted cubes has demonstrated that poor results will be obtained when applying DES to a coarse RANS mesh, which does not account for any expected turbulence structures. The lack of resolution in the shear layer leads to under resolved mixing and hence to a misrepresentation of the Reynolds stresses. These results clearly demand similar resolution requirements for both DES and LES.

From the present results documented in this paper, two main conclusions concerning the applicability of DES can be drawn.

In *internal flows* such as the flow over wall-mounted cubes where a large portion of the domain will be directly influenced by the configuration walls, DES requires almost the same spatial resolution as LES, since DES directly resolves the turbulent structures in most of the flow domain. In this case only the small part close to the wall allows DES to save grid points as it does not require the same fine resolution like a LES to capture

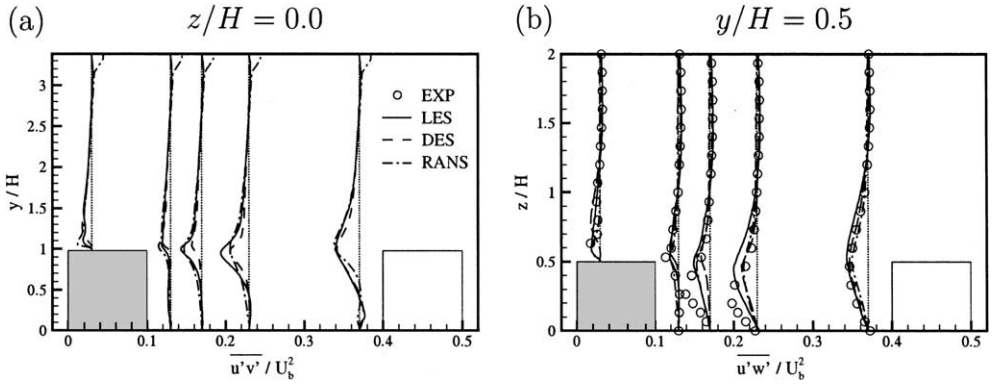

Fig. 7. Reynolds shear stresses $\overline{u_i'u_j'}/U_b^2$ on the z-plane (a) and y-plane (b).

the wall dynamics. This issue becomes even more important at higher Reynolds numbers and in more complex geometries.

The main advantage of DES arises in *external flows*, where usually only a fraction of grid points compared to LES are required, because the transient motion which occur around bodies generally covers a smaller part of the computational domain (e.g. the wake of an airfoil) and does not interact with geometric features such as complex 3D geometries very intensely. As an example, the application of DES to an airfoil configuration (Schmidt and Thiele, 2002) demonstrates the great potential of this new method.

Summarising, it can be expected that, the more the flow contains a substantial amount of unsteady motion, DES will be superior to RANS. However, special care should be taken when creating a mesh for DES in order to account for expected flow patterns in the computational domain. Although the computational effort for an unsteady DES is generally higher than for a typical steady RANS simulation, promising results can be obtained in a reasonable amount of time. From a LES point of view, DES is a way out of the limitation given by resolution constraints, which have to be obeyed by wall-resolving LES and opening up a wide range of industrial related 3D applications.

Acknowledgements

The authors gratefully acknowledge the DFG (Deutsche Forschungsgemeinschaft) for the financial support (SFB 557) and the Konrad-Zuse-Zentrum Berlin (ZIB) for providing the platform and computing time on the Cray-T3E for the calculations underlying this research.

References

Davidson, L., 1997. Large eddy simulation: a dynamic one-equation subgrid model for three-dimensional recirculation flow. In: 11th Symposium on Turbulent shear Flows. Grenoble, France, pp. 26-1–26-6.

Germano, M., Piomelli, U., Moin, P., Cabot, W.H., 1991. A dynamic subgrid-scale eddy viscosity model. Phys. Fluids A 3 (7), 1760–1765.

Hellsten, A., Rautaheimo, P., 1999. Workshop on refined turbulence modelling. Proceedings of the 8th ERCOFTAC/IAHR/COST-Workshop, 17–18 June, 1999, Helsinki, Finland. Helsinki University of Technology.

Lilly, D., 1992. A proposed modification of the Germano subgrid-scale closure method. Phys. Fluids A 4 (3), 633–635.

Lyn, D., Einav, S., Rodi, W., Park, J.H., 1995. A laser-Doppler velocimetry study of ensemble averaged characteristics of the turbulent near wake of a square cylinder. J. Fluid Mech. 304, 285–319.

Meinders, E., 1998. Experimental study of heat transfer in turbulent flows over wall-mounted cubes. Ph.D. Thesis, Delft University of Technology.

Pope, S.B., 2000. Turbulent Flows. Cambridge University Press, Cambridge.

Rhie, C., Chow, W., 1983. Numerical study of the turbulent flow past an airfoil with trailing edge separation. AIAA J. 21 (11), 1525–1532.

Rodi, W., Ferziger, J., Breuer, M., Pourquié, M., 1997. Status of large eddy simulation: results of a workshop. J. Fluids Eng. 119 (6), 248–262.

Schmidt, S., 2000. Grobstruktursimulation turbulenter Strömungen in komplexen Geometrien und bei hohen Reynoldszahlen (Large-eddy simulation of turbulent flows in complex geometries and at high Reynolds numbers). Mensch Mensch & Buch Verlag, Berlin, ISBN 3-89820-185-6 (in German).

Schmidt, S., Lübcke, H., Thiele, F., 1999. Comparison of LES and RANS for bluff-body wake flows. Poster presentation, GAMM-Workshop, Kirchzarten, September, Germany.

Schmidt, S., Thiele, F., 2002. Detached and large eddy simulation of airfoil flow on semi-structured grids. In: Friedrich, R., Rodi, W. (Eds.), Proceedings of the EUROMECH Colloquium 412, Munich, 4–6 October, 2000. Kluwer Academic Publishers, Dordrecht.

Shur, M., Spalart, P., Strelets, M., Travin, A., 1999. Detached-eddy simulation of an airfoil at high angle of attack. In: Rodi, W., Laurence, D. (Eds.), Turbulent Shear Flows. Elsevier Science, Amsterdam, pp. 669–678.

Smagorinsky, J., 1963. General circulation experiments with the primitive equations. Monthly Weather Rev. 91, 99–164.

Sohankar, A., Davidson, L., Norberg, C., 2000. Large eddy simulation of flow past a square cylinder: comparison of different subgrid scale models. J. Fluids Eng. 122, 39–47.

Spalart, P., Allmaras, S., 1994. A one-equation turbulence model for aerodynamic flows. La Rech. Aérospatiale 1, 5–21.

Spalart, P., Jou, W.H., Strelets, M., Allmaras, S., 1997. Comments on the feasibility of LES for wings, and on a hybrid RANS/LES approach. In: Liu, C., Liu, Z. (Eds.), Advances in DNS/LES. Greyden Press.

Driest, E., 1956. On turbulent flow near a wall. J. Aero. Sci. 23, 1007–1011.

Wilcox, D.C., 1993. Turbulence modeling for CFD. DCW Industries.

Xue, L., 1998. Entwicklung eines effizienten parallelen Lösungsalgorithmus zur dreidimensionalen Simulation komplexer turbulenter Strömungen. Dissertation, Technische Universität Berlin.